Diffractive shadowing of coherent polarization radiation

A. Curcio, M. Bergamaschi, R. Corsini, D. Gamba, W. Farabolini, R. Kieffer, T. Lefevre, and S. Mazzoni
CERN, CH-1211 Geneva 23, Switzerland

V. Dolci and M. Petrarca
Department of Basic and Applied Sciences for Engineering (SBAI) and INFN-Roma1, "Sapienza" University of Rome, Via A. Scarpa 14, 00161 Rome, Italy

P. Karataev
John Adams Institute at Royal Holloway, University of London, Egham, Surrey, TW20 0EX, UK

K. Lekomtsev
National Research Nuclear University MEPhI (Moscow Engineering Physics Institute), Kashirskoe Highway, 31, Moscow 115409, Russian Federation and John Adams Institute at Royal Holloway, University of London, Egham, Surrey, TW20 0EX, UK

S. Lupi
Physics Department of University of Rome "La Sapienza" and INFN-Roma1, Piazzale Aldo Moro 5, 00185 Rome, Italy

A. Potylitsyn
Tomsk Polytechnic University, 634050, Lenin Ave, Tomsk, Russia
(Dated: December 3, 2020)

We report on the study of shadowing of electromagnetic fields radiated in the Terahertz (THz) region from two consecutive sources of coherent diffraction and transition radiation. In these conditions, the formation length is predicted to be $\lesssim 100\ m$, and shadowing effects should result in an almost complete suppression of radiated fields within distances of the order of tens of centimeters. We experimentally measured that shadowing effects disappear for distances significantly shorter than those predicted. We propose a new model that explains our experimental observations by taking into account 3D diffraction effects. These findings will have a positive impact on the beneficial use of consecutive radiators both for the generation of intense electromagnetic radiation and for beam diagnostics using coherent polarization radiation from ultra-relativistic charged particles.

Polarization radiation refers to the emission of electromagnetic radiation during the interaction of charged particles with a dielectric medium, and typically includes well-known radiation mechanisms such as Transition [1] and Diffraction radiation [2], Smith-Purcell radiation [3] and Cherenkov radiation [4]. In many configurations the radiation is emitted by several sources, where any edge, aperture and in general any electrically-polarizable medium or surface may become a source of radiation in presence of high energy/high current beams of charged particles. In particles' accelerators multiple sources could be provided by metallic and dielectric components placed nearby the beams, moreover synchrotron radiation emitted in bending magnets should also be considered. In its simplest form a system of multiple sources will just consist of two consecutive foils. The resulting radiation pattern can be explained by the interference between the forward transition radiation from the first foil (i.e. propagating along the particle trajectory) with the backward transition radiation emitted by the second foil (i.e. along the direction of specular reflection from the surface). Garibyan in [5, 6] introduced the concept of formation length L_f that is the distance over which the phase difference between the radiation field and the particle field is 1 rad, defined as

$$L_f = \frac{\lambda\beta}{2\pi(1-\beta\cos\theta)} \quad (1)$$

where β is the normalized velocity of the particle along the travel direction, related to the Lorentz factor $\gamma = (1-\beta^2)^{-1/2}$. The radiation wavelength is λ, θ is the polar observation angle. For relativistic particles, the formation length of forward transition radiation is $L_f \sim \gamma^2\lambda/2\pi$ and can extend to large distances. For the backward transition radiation, it reduces typically to a fraction of λ [7]. It is thus predicted that the total emitted power from two consecutive sources is optimal if the distance between them is longer than L_f, whereas destructive interference would occur for distances z shorter than L_f resulting in a strong reduction of the total radiation intensity. Experimentally, radiation from two consecutive metallic foils with z/L_f larger than 1.2 was studied in the pioneering work of Wartski [8] on Optical Transition Radiation Interference (OTRI) using 70 MeV electrons. Shadowing in the optical range was studied in detail in [9] using 200 MeV electrons and z/L_f as small as 0.05. This study confirmed the presence of a strong destructive interference as expected by theoretical predictions [10]. The emission of coherent polarization radiation from short electron bunches has demonstrated its potential as a source of high power radiation in the sub-THz to THz range [11–14], and has also found applications for beam instrumentation purposes [15, 16] and spectroscopy. Observations of shadowing were performed by Naumenko [17],[18] measuring coherent radiation emitted at $\lambda = 10\ mm$ by 6.1 MeV electron bunches. In that configuration, the predicted formation length was about 0.45 m long, and they observed a reduction of a factor 5 in radiation power for z ranging from 22 cm to 2 cm. This reduction was smaller than the value predicted by shadowing theory (i.e. > 10) but still considered by the authors as an acceptable agreement, once taken into account experimental uncertainties.

In this letter we report on the study of shadowing effects occurring in the THz range between two sources of coherent radiation based on Coherent Diffraction Radiation (CDR) and Coherent Transition Radiation (CTR). The experiments were performed at the Cern Linear Electron Accelerator for Research (CLEAR) using relativistic short electron bunches. We then present a new general formalism that can model the interference mechanism between two consecutive coherent sources and accurately simulate shadowing effects in diffractive conditions. The CLEAR facility [19] delivers electron bunches

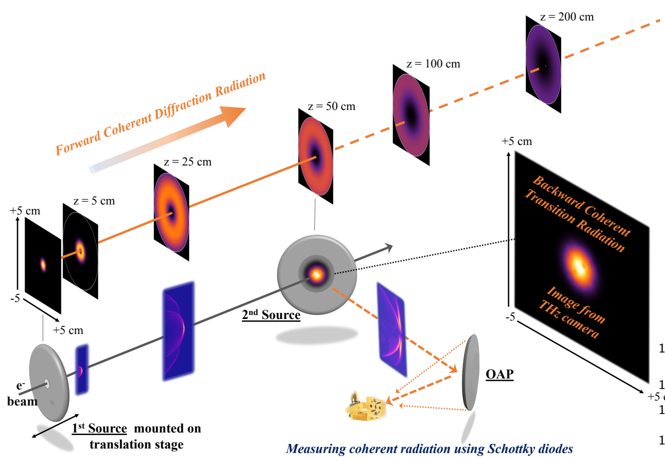

Figure 1. Experimental set-up at CLEAR : the electron beam e^- emits forward CTR/CDR from a first screen that interferes with backward CTR from a second screen. The resulting coherent radiation pulse is collected by an Off-Axis Parabolic (OAP) mirror that focuses it towards the detector.

with maximal beam energy of 200 MeV. A 1 m-long in-air testing area has been installed at the end of the beamline for the study of THz generation using coherent radiation mechanisms [16, 19]. The experimental set-up installed on CLEAR to study the shadowing effect of coherent radiation is composed of two consecutive sources emitting transition or diffraction radiation, as depicted in Fig. 1. A first screen placed perpendicular to the beam trajectory, produces forward coherent radiation. It is mounted on a remotely controlled translation stage allowing the precise adjustment of the distance between the two sources from 5 cm to 45 cm. Snapshots of the spatial distribution of the forward coherent radiation emitted from the first radiator are shown in Fig. 1 as an example. The resulting forward coherent radiation propagates co-linearly with the beam towards the second source. The latter is a screen tilted at 45° that emits backward CTR and reflects the forward radiation emitted from the first source. Both screens are made out of silicon, 0.4 mm thick, coated with a 0.1 mm thick aluminum layer and with an external radius of 50 mm. The corresponding radiation, whose front is figured as result of a 3D simulations using the VSim code [20], is collected by an Off-Axis Parabolic (OAP) mirror (focal length of 15.4 cm), positioned 20 cm away from the second screen, focusing the radiation on the detection plane. The measurement system is based on waveguide band-pass-filtered Schottky diodes from *Millitech*. Two ini-

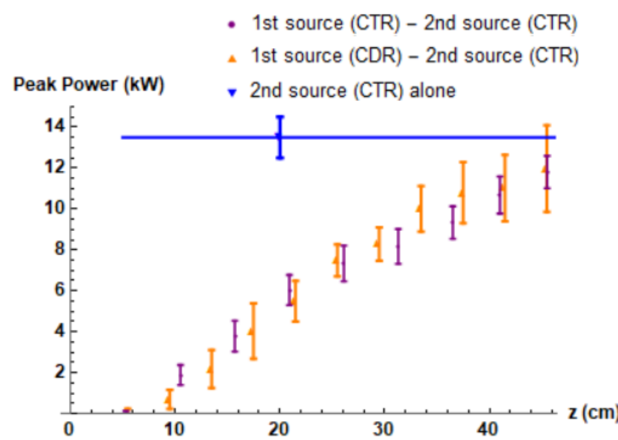

Figure 2. Measured radiation power at $\lambda = 1.76\ mm$ as a function of the distance between the two sources. The blue line represents the measured power of backward CTR emitted by the second source alone.

tial tests have been carried out with electron bunches of 200 MeV and 1.5 ps rms long, using as first source of radiation either a solid screen or a hollow screen with 5 mm internal radius hole, emitting forward coherent transition or diffraction radiation respectively. In those first tests the radiation output power has been measured at a wavelength of $\lambda = 1.76\ mm$, and its evolution as a function of the distance between sources, z, is depicted in Fig. 2. The error has been evaluated as the rms fluctuation of the signal. In both cases a strong shadowing effect is observed for small values of z (i.e. 5 cm) and the radiation power rapidly increases for larger distances between the sources. This observation is in direct contradiction with the model described by Eq. 1, which would predict a formation length in the $\lesssim 100\ m$ range, suggesting a much stronger shadowing for $z = 45\ cm$. Whether the first source emits CTR or CDR has also a negligible impact on measured output powers and the corresponding shadowing effects. This suggests that the diffraction effect occurring at the central hole of the first screen is modifying very weakly the properties of the emitted forward coherent radiation. For the maximum value $z = 45\ cm$ the measured power reaches a level equivalent to the one corresponding to the emission of backward CTR from a single screen. This power is represented in Fig. 2 by the blue line. An image of the backward CTR radiation pattern acquired using a THz camera, is depicted in Fig 1 and shows that the CTR source has a size of 3 mm rms. Complementary investigations have been performed to study the dependency of shadowing effects with respect to the beam energy and the observation wavelength. In those measurements the hollow screen emitting forward CDR has been kept as the first source of radiation. With 200 MeV electrons the radiation power has been acquired in two frequency bands, using band-pass-filtered Schottky diodes at $0.100 \pm 0.009\ THz$ and $0.170 \pm 0.009\ THz$ (i.e. $\lambda = 2.99\ mm$ and $\lambda = 1.76\ mm$). The results presented in Fig. 3(a) show a slightly stronger shadowing for longer wavelength, which is not in contradiction with the theory expressed by Eq. 1, that foresees a dependency proportional to λ. The additional experimental results obtained for different electron energies are presented in Fig. 3(b). A small dependence on beam energy is measured, with shadowing effects slightly reducing for lower beam energies. This observation is in contradiction with the model described by Eq. 1 that predicts a much stronger dependency with beam energies, proportional to γ^2. In comparison, for shorter wavelength in the optical range, the light emission from two consecutive transition radiation screens is doubling for large distance between sources [9]. Furthermore, the data in Fig. 3 has been normalized to the reference level $\sim 13.5\ kW$, which was comparable (within the error bars) to the one measured in the experiment reported by Fig. 2 both for different wavelengths and for different beam energies, due to the experimental setup affected by diffraction losses dominating both the radiation production and its detection.

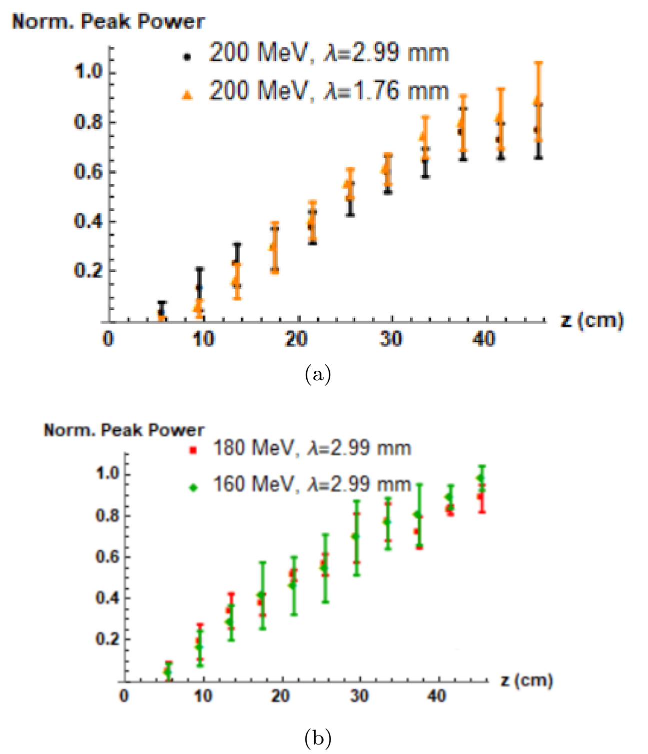

Figure 3. Top **(a)**: Normalized radiation power as a function of the distance between the two sources of CDR and CTR, at different radiation wavelengths. Bottom **(b)**: Normalized radiation power as a function of the distance between the two sources of CDR and CTR, at different beam energies.

All those observations indicate that the correct modelling of shadowing effects in the sub-THz range requires a more detailed treatment than the one developed initially for short wavelengths. Theoretically, the electric field of forward CTR or CDR radiated by ultra-relativistic electrons can be calculated using the formalism developed in [21] or [22]. For an azimuthally symmetric geometry and for a gaussian electron bunch with rms time-duration σ_τ, the electric field radiated forward from a round and perfectly conducting disk with an external radius b and a central hole with radius a is described by the radial polarization component

$$E_f(\vec{R},\omega) = \frac{iQ\omega^2 e^{i\frac{\omega R}{c} - \frac{\omega^2\sigma_\tau^2}{2}}}{4\pi\varepsilon_0\beta^2\gamma c^2 R} \times \\ \times \left[\int_a^b d\varrho \varrho K_1\left(\frac{\omega\varrho}{\beta\gamma c}\right) J_1\left(\frac{\omega\varrho}{c}\sin\theta\right) e^{\frac{i\omega\varrho^2}{2cR}} \right] \tag{2}$$

where Q is the total charge of the electron bunch, c is the speed of light in vacuum, $\omega = 2\pi c/\lambda$ is the angular frequency of radiation, φ is the azimuthal angle, and ε_0 is the vacuum dielectric constant. When $a = 0$ and $b \to \infty$, Eq. 2 corresponds to the field radiated by ideal transition radiation. In addition, the diffraction effect from the hole is small, and the CDR field distributions become similar to the ones of CTR as it is observed experimentally and reported in Fig. 2. This concept is generally true in our case because even the outer target dimensions are much smaller than the field radius. We define the observation-distance vector $\vec{R} = R\{\cos\varphi\sin\theta, \sin\varphi\sin\theta, \cos\theta\}$, with $R = (x^2 + y^2 + z^2)^{1/2}$. The spectral-angular distribution of forward radiated energy is obtained from Eq. 2 using

$$\frac{d^2 I}{d\omega d\Omega} = \frac{\mu_0 c}{\pi} \left| E_f(\vec{R},\omega) \right|^2 R^2 \tag{3}$$

Equations 2 and 3 show that the angular distribution of the radiation changes as a function of the distance from the source, z. Studied by Verzilov in [23], this feature is due to the so-called pre-wave zone effect, and reflects the fact that the radiated field is not a point source but expands transversely similarly to the particle field. The angular distribution of the radiation is thus affected by the transverse distribution of the particle beam at least for small distances z from the source, as was also shown in simulations in [24]. Only in the far-field zone, for $z >>$

$\gamma^2\lambda/2\pi$, such a dependence disappears. Using Eq. 2 the angular distribution of forward coherent radiation can be calculated as a function of z. Several examples of such distribution are depicted in Fig. 4 for the wavelengths $\lambda = 1.76$ and 2.99 mm, assuming electrons with $\gamma = 400$ and a screen with parameters $a = 5$ mm and $b = 50$ mm. The peak of the angular distribution of forward CDR, changes significantly as a function of the distance from the source as expected from both diffraction and pre-wave zone effects. For relatively short distances from the source, the emission cone of the radiation θ_d is large and decreases asymptotically with z to reach a value of $\theta_d \sim 0.38\lambda/b$ [25]. The shadowing effect between two

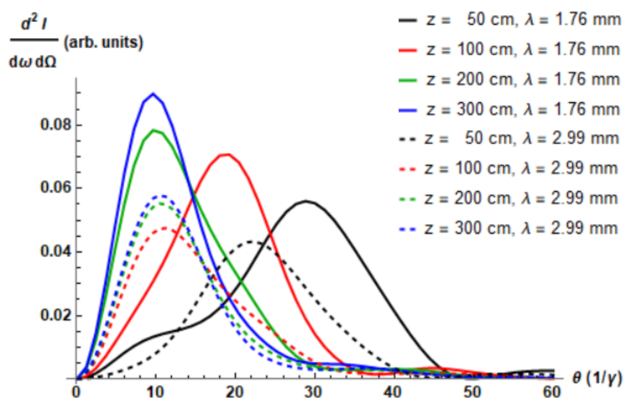

Figure 4. Angular distribution of forward CDR for different distances from the source and for two different wavelengths.

consecutive sources can be calculated by summing up the spatial distribution of the forward CDR field, emitted from the first screen and propagating to the position of second screen, with the backward CTR field emitted by the latter. The total field is thus written as follows

$$\vec{E}(\vec{r},\omega) = P(\vec{r},\omega)\vec{E}_f(\vec{r},\omega)e^{iz/L_f} + \vec{E}_b(\vec{r},\omega) \qquad (4)$$

where P is the pupil function taking into account the limited size of the second radiator with respect to the diverging front of forward radiation. The field $\vec{E}_b$ is obtained from Eq. 2, sending $\cos\theta \to -\cos\theta$ and $a \to 0$. Using this formalism, calculations have been performed to reproduce the experimental data. The results are presented in Fig. 5. The calculations have been carried out considering exactly the same parameters used for the experiment, both in terms of beam parameters and setup geometry. The data and the calculations have been consistent within the error bars associated to the experiment. More precise measurements could have matched even better the analytic model, nevertheless the electron charge fluctuations during the experiment have determined non-negligible fluctuations of the intensity of the coherent light and the goodness of the results has been slightly affected by this experimental limitation. The new model above presented is certainly an extension of the previous one used for example in [9], where incoherent radiation was considered and no diffraction effects were

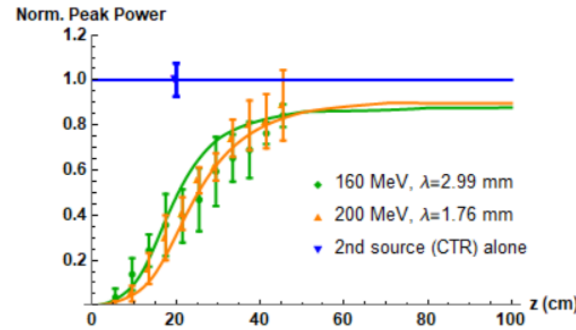

Figure 5. Comparison between data and analytic calculations for the shadowing of coherent radiation. Blue line corresponding to 13.5 kW.

taken into account. Indeed, Eq. 2 contains this new information, since the gaussian term in the radiation frequency is related to the bunch form factor (coherent radiation) and the expression under the integration sign is a Fresnel integral (diffraction effects). For sake of coherence and completeness we have also introduced the pupil function in Eq. 4 which takes into account the diffraction losses of the forward radiation front propagating onto the surface of the second radiator (where there was no need for this in previous works with incoherent radiation). It's important to state that, doing so, the analytic calculations only consider the diffraction losses but not the deformation of the reflected wavefronts due to the diffraction. Finally this aspect has not been so relevant for the presented experiment because the expected diffraction angle was low $\lambda/b << 1$ and also because the detection has been performed by integrating over the radiation wavefronts, measuring only the total power. In the (sub-)THz range and for ultra relativistic electrons, several key parameters need to be considered to understand shadowing effects correctly and to estimate the output radiated power quantitatively. First, the interference becomes predominantly sensitive to the spatial overlap between the two radiation fields at the position of the second source. Secondly, the typical approximation of an infinitely wide radiator, used for short wavelengths, becomes invalid as the transverse dimension of the beam field is typically larger than the source size defined by the outer target dimensions, i.e. $\gamma\lambda >> b$ for longer wavelengths. This dependence of the spectral-angular distribution of the coherent radiation on the external radius of the radiator b has been experimentally studied in [26]. In order to estimate how important these two effects are on shadowing, further calculations have been made using infinitely large radii for the first and the second source, b_1 and b_2, where we consider that the radius of the OAP mirror is infinite when the radius of the second source is also infinite. The results, plotted in Figs. 6(a) and 6(b), show a strong effect of the source radius on shadowing. When b_1 is infinite while $b_2 = 50$ mm shadowing effects increase and the output radiation levels decrease

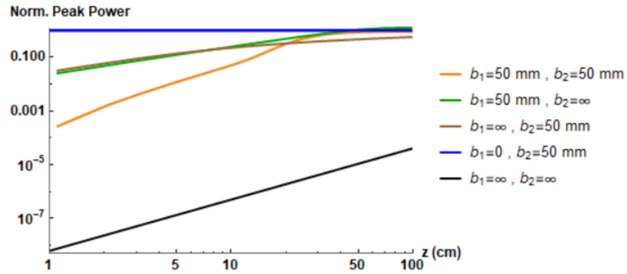

(a)

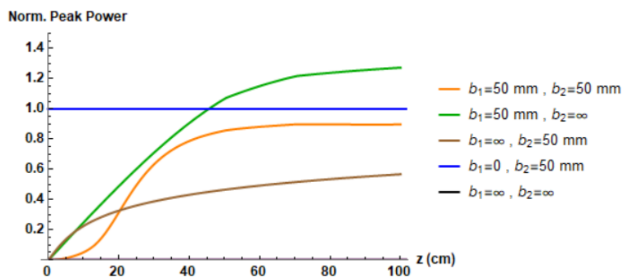

(b)

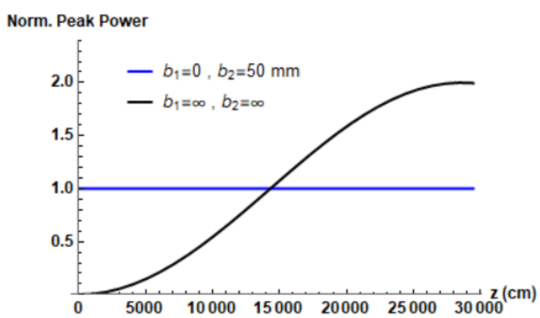

(c)

Figure 6. Top **(a)**: Simulated shadowing effect with two sources of different size (peak power normalized to the case $b_1 = 0, b_2 = 50\ mm$). Center **(b)**: Linear scale of the same plot in Fig. 6(a) . Bottom **(c)**: The limit case $b_1 = \infty, b_2 = \infty$, normally valid with inchoerent radiation.

by roughly 40 % of the level of the backward CTR alone. In the opposite case, with $b_1 = 50\ mm$ and b_2 infinite, the shadowing effect would decrease with the corresponding output power higher by 30 %. One should also note that backward CTR power from an infinite large radiator is expected to be larger by a factor > 3 compared to the value obtained in our test for a 50 mm radius source. For completeness, the hypothetical case with all sources having an infinite radius is also presented in Fig. 6(c), where the shadowing effect would be much stronger. For a distance $> 300\ m$ the radiation would reach a level corresponding to twice the output power emitted as CTR from a single source, thus matching the observation done by [9] for shorter wavelengths with a formation length as long as one hundred meters. Fig. 6 demonstrates that even if the observations made with coherent radiation might seem in contradiction with past observations made with incoherent radiation, when properly considering the diffraction effects, one situation reduces to the other continuously, therefore the diffractive shadowing of coherent radiation is only a natural extension of the shadowing of incoherent radiation. The authors have found as well much instructive to represent examples of shadowing for limit situations as infinite radiators, finite radiators and mixed combinations.

In conclusion, we have been experimentally studying the shadowing effect between two sources of coherent radiation. We complemented our observations by the development of a generalized formalism that enables to accurately predict shadowing effects in diffractive conditions. For longer wavelength (i.e. mm) and relativistic beam energies $\gamma >> 1$, diffraction effects and pre-wave zone effects play a crucial role in the interference mechanism between two consecutive sources of radiation. The physical sizes of those sources are key parameters that influence the electromagnetic shadowing and limit its effect to a short distance. Our results will benefit any application of coherent radiation from multiple consecutive sources for intense THz beam generation [27–29] or for beam diagnostics' purposes [30], where an upstream screen is used to shield from coherent radiation background such as synchrotron radiation or wakefields.

A.Potylitsyn's contribution was supported by Tomsk Polytechnic University CE Program.

K. Lekomtsev's contribution was supported by the Competitiveness Programme of National Research Nuclear University "MEPhI and by the Ministry of Education and Science of the Russian Federation, project № 0723-2020-0037."

---

[1] V. Ginzburg and I. Frank, Radiation of a uniformly moving electron due to its transition from one medium into another, Zh. Eksp. Teor. Fiz. **9**, 353 (1945).

[2] A. P. Potylitsyn, Transition radiation and diffraction radiation. similarities and differences, Nuclear Instruments and Methods in Physics Research Section B: Beam Interactions with Materials and Atoms **145**, 169 (1998).

[3] S. J. Smith and E. Purcell, Visible light from localized surface charges moving across a grating, Physical Review **92**, 1069 (1953).

[4] P. Čerenkov, Visible radiation produced by electrons moving in a medium with velocities exceeding that of light, Physical Review **52**, 378 (1937).

[5] G. Garibyan, Radiation from a charged particle passing through a layered medium, Journal of Experimental and Theoretical Physics **6**, 1079 (1958).

[6] G. Garibyan, Transition radiation effects in particle energy losses, Soviet Physics JETP **37**, 2 (1960).

[7] X. Artru, R. Chehab, K. Honkavaara, and A. Variola, Resolution power of optical transition radiation: Theoretical considerations, Nuclear Instruments and Methods in Physics Research Section B: Beam Interactions with Materials and Atoms **145**, 160 (1998).

[8] L. Wartski, S. Roland, J. Lasalle, M. Bolore, and G. Filippi, Interference phenomenon in optical transition radiation and its application to particle beam diagnostics and multiple-scattering measurements, Journal of Applied Physics **46**, 3644 (1975).

[9] R. Kieffer, M. Bergamaschi, E. Bravin, W. Farabolini, P. Karataev, T. Lefevre, and S. Mazzoni, Experimental observation of "shadowing" in optical transition radiation, Physical review letters **120**, 094802 (2018).

[10] X. Artru and C. Ray, Interference and shadow effects in the production of light by charged particles in optical fibers, Nuclear Instruments and Methods in Physics Research Section B: Beam Interactions with Materials and Atoms **266**, 3725 (2008).

[11] Y. Honda, M. Shimada, A. Aryshev, R. Kato, T. Miyajima, T. Obina, R. Takai, T. Uchiyama, and N. Yamamoto, Stimulated excitation of an optical cavity by a multibunch electron beam via coherent-diffraction-radiation process, Physical review letters **121**, 184801 (2018).

[12] E. Chiadroni, A. Bacci, M. Bellaveglia, M. Boscolo, M. Castellano, L. Cultrera, G. Di Pirro, M. Ferrario, L. Ficcadenti, D. Filippetto, *et al.*, The sparc linear accelerator based terahertz source, Applied Physics Letters **102**, 094101 (2013).

[13] E. Chiadroni, M. Bellaveglia, P. Calvani, M. Castellano, L. Catani, A. Cianchi, G. Di Pirro, M. Ferrario, G. Gatti, O. Limaj, *et al.*, Characterization of the thz radiation source at the frascati linear accelerator, Review of Scientific Instruments **84**, 022703 (2013).

[14] A. Perucchi, S. Di Mitri, G. Penco, E. Allaria, and S. Lupi, The terafermi terahertz source at the seeded fermi free-electron-laser facility, Review of Scientific Instruments **84**, 022702 (2013).

[15] M. Veronese, R. Appio, P. Craievich, and G. Penco, Absolute bunch length measurement using coherent diffraction radiation, Physical review letters **110**, 074802 (2013).

[16] A. Curcio, M. Bergamaschi, R. Corsini, W. Farabolini, D. Gamba, L. Garolfi, R. Kieffer, T. Lefevre, S. Mazzoni, K. Fedorov, *et al.*, Noninvasive bunch length measurements exploiting cherenkov diffraction radiation, Physical Review Accelerators and Beams **23**, 022802 (2020).

[17] G. A. Naumenko, A. P. Potylitsyn, L. G. Sukhikh, Y. A. Popov, and M. Shevelev, Macroscopic effect of the shadow of the electromagnetic field of relativistic electrons, JETP letters **90**, 96 (2009).

[18] G. Naumenko, X. Artru, A. Potylitsyn, Y. Popov, L. Sukhikh, and M. Shevelev, " shadowing" of the electromagnetic field of relativistic charged particles, in *Journal of Physics: Conference Series*, Vol. 236 (IOP Publishing, 2010) p. 012004.

[19] A. Curcio, M. Bergamaschi, R. Corsini, D. Gamba, W. Farabolini, T. Lefevre, S. Mazzoni, V. Dolci, M. Petrarca, and S. Lupi, Beam-based sub-thz source at the cern linac electron accelerator for research facility, Physical Review Accelerators and Beams **22**, 020402 (2019).

[20] C. Nieter and J. R. Cary, Vorpal: a versatile plasma simulation code, Journal of Computational Physics **196**, 448 (2004).

[21] D. Karlovets and A. Potylitsyn, Universal description for different types of polarization radiation, arXiv preprint arXiv:0908.2336 (2009).

[22] K. Lekomtsev, G. Blair, G. Boorman, R. Corsini, P. Karataev, T. Lefevre, and M. Micheler, Coherent diffraction radiation experiment at ctf3—simulation studies, Il nuovo cimento C **34**, 261 (2011).

[23] V. Verzilov, Transition radiation in the pre-wave zone, Physic Letters A **275**, 135 (2000).

[24] T. Aumeyr, M. G. Billing, L. M. Bobb, B. Bolzon, P. Karataev, T. Lefevre, and S. Mazzoni, Zemax simulations of transition and diffraction radiation, in *Journal of Physics: Conference Series*, Vol. 517 (IOP Publishing, 2014) p. 012026.

[25] A. Potylitsyn, Image of optical diffraction radiation (odr) source and spatial resolution of odr beam profile monitor, in *Advanced Radiation Sources and Applications* (Springer, 2006) pp. 149–163.

[26] M. Castellano, V. Verzilov, L. Catani, A. Cianchi, G. Orlandi, and M. Geitz, Measurements of coherent diffraction radiation and its application for bunch length diagnostics in particle accelerators, Physical Review E **63**, 056501 (2001).

[27] N. Sei and T. Takahashi, first demonstration of coherent resonant backward diffraction radiation for a quasi-monochromatic terahertz-light source, Scientific Reports **10**, 1 (2020).

[28] T. Pacey, Y. Saveliev, A. Healy, P. Huggard, B. Alderman, P. Karataev, K. Fedorov, and G. Xia, Continuously tunable narrow-band terahertz generation with a dielectric lined waveguide driven by short electron bunches, Physical Review Accelerators and Beams **22**, 091302 (2019).

[29] A. Aryshev, S. Araki, M. Fukuda, P. Karataev, A. Konkov, G. Naumenko, A. Potylitsyn, K. Sakaue, L. Sukhikh, N. Terunuma, *et al.*, Observation of the stimulated coherent diffraction radiation in an open resonator at lucx facility, Nuclear Instruments and Methods in Physics Research Section A: Accelerators, Spectrometers, Detectors and Associated Equipment **763**, 424 (2014).

[30] K. Lekomtsev, G. Boorman, R. Corsini, P. Karataev, and T. Lefevre, Investigation of coherent diffraction radiation from a dual target system at ctf3, in *Journal of Physics: Conference Series*, Vol. 357 (IOP Publishing, 2012) p. 012021.